PGC-1α, A Potential Therapeutic Target for Early Intervention in Parkinson's Disease

Bin Zheng[1], **Zhixiang Liao**[1], **Joseph J. Locascio**[2], **Kristen A. Lesniak**[3], **Sarah S. Roderick**[1], **Marla L. Watt**[3], **Aron C. Eklund**[1,4], **Yanli Zhang-James**[5], **Peter D. Kim**[6], **Michael A. Hauser**[7], **Edna Grünblatt**[8], **Linda B. Moran**[9], **Silvia A. Mandel**[10], **Peter Riederer**[8], **Renee M. Miller**[11], **Howard J. Federoff**[12], **Ullrich Wüllner**[13], **Spyridon Papapetropoulos**[14,15], **Moussa B. Youdim**[10,16], **Ippolita Cantuti-Castelvetri**[2], **Anne B. Young**[2], **Jeffery M. Vance**[17], **Richard L. Davis**[18], **John C. Hedreen**[19], **Charles H. Adler**[20], **Thomas G. Beach**[21], **Manuel B. Graeber**[22], **Frank A. Middleton**[18], **Jean-Christophe Rochet**[3], **Clemens R. Scherzer**[1,23,*], and **the Global PD Gene Expression (GPEX) Consortium**

[1] Laboratory for Neurogenomics, Center for Neurologic Diseases, Harvard Medical School and Brigham and Women's Hospital, 65 Landsdowne Street, Suite 307A, Cambridge, MA 02139, USA

[2] Department of Neurology, Massachusetts General Hospital, Boston, MA 02114, USA

[3] Department of Medicinal Chemistry and Molecular Pharmacology, Purdue University, West Lafayette, IN 47907, USA

[4] Center for Biological Sequence Analysis, Department of Systems Biology, Technical University of Denmark, 2800 Lyngby, Denmark

[5] Department of Psychiatry, SUNY Upstate Medical University, Syracuse, NY 13210, USA

[6] Department of Neurosurgery, SUNY Upstate Medical University, Syracuse, NY 13210, USA

[7] Department of Medicine, Duke University, Durham, NC 27708, USA

[8] Clinical Neurochemistry, National Parkinson Foundation Centre of Excellence Research Laboratory, University of Würzburg, 97070 Würzburg, Germany

[9] North Wembley, Middlesex, HAO 3QJ, UK

[*]Correspondence should be addressed to C.R.S., Clemens R. Scherzer, M.D., Laboratory for Neurogenomics, Center for Neurologic Diseases, Harvard Medical School and Brigham & Women's Hospital, 65 Landsdowne Street, Suite 307A, Cambridge, MA 02139, Phone: 617-768-8427, Fax: 617-768-8595, cscherzer@rics.bwh.harvard.edu.

[10] Eve Topf and National Parkinson Foundation Centers of Excellence for Neurodegenerative Diseases, Technion-Faculty of Medicine, Haifa 31096, Israel

[11] Center for Neural Development and Disease, University of Rochester, Rochester, NY 14620, USA

[12] Department of Neurology, Georgetown University Medical Center, Washington, DC 20007, USA

[13] Department of Neurology, Friedrich-Wilhelms-University Bonn, UKB, 53105 Bonn, Germany

[14] Department of Neurology, Miller School of Medicine, University of Miami, Miami, FL 33136, USA

[15] Allergan, Irvine, CA 92623-9534, USA

[16] Department of Biology, Yonsei World Central University, Department of Biology, Seoul 120-749, South Korea

[17] Hussman Institute for Human Genomics, Miller School of Medicine, University of Miami, Miami, FL 33136, USA

[18] Department of Pathology, SUNY Upstate Medical University, Syracuse, NY 13210, USA

[19] Harvard Brain Tissue Resource Center, Department of Psychiatry, McLean Hospital, Belmont, MA 02478, USA

[20] Mayo Division of Movement Disorders, Mayo Clinic Arizona, Scottsdale, AZ 85259, USA

[21] W. H. Civin Laboratory of Neuropathology, Sun Health Research Institute, Sun City, AZ 85259, USA

[22] The Brain & Mind Research Institute, University of Sydney, Sydney, NSW 2050, Australia

[23] Harvard NeuroDiscovery Center Biomarker Program, Cambridge, MA 02139, USA

Abstract

Parkinson's disease affects 5 million people worldwide, but the molecular mechanisms underlying its pathogenesis are still unclear. Here, we report a genome-wide meta-analysis of gene sets (groups of genes that encode the same biological pathway or process) in 410 samples from patients with symptomatic Parkinson's and subclinical disease and healthy controls. We analyzed 6.8 million raw data points from nine genome-wide expression studies, and 185 laser-captured human dopaminergic neuron and substantia nigra transcriptomes, followed by two-stage replication on three platforms. We found 10 gene sets with previously unknown associations with Parkinson's disease. These gene sets pinpoint defects in mitochondrial electron transport, glucose utilization, and glucose sensing and reveal that they occur early in disease pathogenesis. Genes controlling cellular bioenergetics that are expressed in response to peroxisome proliferator–activated receptor γ coactivator-1α (*PGC-1α*) are underexpressed in Parkinson's disease patients. Activation of *PGC-1α* results in increased expression of nuclear-encoded subunits of the mitochondrial respiratory chain and blocks the dopaminergic neuron loss induced by mutant α-synuclein or the pesticide rotenone in cellular disease models. Our systems biology analysis of Parkinson's disease identifies *PGC-1α* as a potential therapeutic target for early intervention.

Keywords

receptor-gamma coactivator 1 alpha (*PPARGC1A)*; α-synuclein; *PINK1*; parkin; mitochondria; oxidative phosphorylation; glucose utilization; complex I

INTRODUCTION

Parkinson's disease (PD) is a genetically complex, neurodegenerative disease with a significant but small genetic risk. In patients with PD, movement, sleep, autonomic functions, and cognition become progressively impaired. Degeneration of dopamine neurons in the substantia nigra of the brain and α-synuclein–positive Lewy bodies in brainstem and neocortex are found at autopsy, but the underlying etiology of the disease is not known.

Both environmental chemicals and genetic susceptibility are thought to contribute to the etiology of sporadic PD. Epidemiological research indicates that exposure to pesticides including rotenone (1), and welding elevates risk of PD (2). The pesticide rotenone inhibits complex I [proton pumping NADH (reduced form of nicotinamide adenine dinucleotide):ubiquinone oxidoreductase] of the mitochondrial respiratory chain in dopaminergic cells (3, 4) and reproduces many of the features of PD including α-synuclein inclusions in rats (5). Intravenous injection of another complex I inhibitor, 1,2,3,6-methyl-phenyl-tetrahydropyridine (MPTP), a contaminant in synthetic opiates, causes acute, permanent parkinsonism and dopamine neuron death in humans (6). By contrast, caffeine and tobacco are associated with reduced risk of PD (2).

Although most PD cases are sporadic, the discovery of genes linked to rare familial forms of disease due to mutations in the *SNCA* (α-synuclein), *PARK2*, *DJ-1*, *PINK1* and *LRRK2* genes has provided important clues about the disease process (7). Loss-of-function mutations in two genes linked to autosomal recessive PD - the nuclear-encoded mitochondrial gene *PINK1* [PTEN (phosphatase and tensin homolog)-induced putative kinase-1] (8) and the E3 ubiquitin ligase *PARK2* - disrupt mitochondrial function (9). Overexpression of *SNCA* carrying the familial PD-linked A53T mutation inhibits mitochondrial complex I in dopaminergic cells (10). In the common sporadic disease, α-synuclein and degenerating mitochondria (11) are major components of Lewy bodies—the hallmark cytoplasmic inclusions found in patient brains—and biochemical complex I deficiency is found in the substantia nigra and in platelets (7).

Massively parallel analysis of messenger RNA (mRNA) transcripts can provide an unbiased, global estimate of changes in gene expression and identify genes (12, 13) and pathways causally, reactively, or independently associated with genetic, environmental, or complex disease etiologies (13, 14). Gene expression data can be used to classify individuals according to molecular characteristics (15) and to generate hypotheses about disease mechanisms (16), and may be particularly useful for decoding complex diseases with considerable environmental and epigenetic contributions not readily explained by variations in DNA sequence. In practice, the power of genome-wide expression technology has been encumbered by discordant analyses, nonreplication, and small sample sizes typical of human studies. This problem is sharply brought into focus by studies of substantia nigra, a small region in the brainstem particularly vulnerable to PD, for which only very limited numbers of high-quality, snap-frozen, postmortem samples are globally available.

Here, we have analyzed variation in expression of multiple members of one molecular pathway (groups of genes that encode a biological process), with the power afforded by random-effects model meta-analysis of 17 studies (five previously unpublished), including analysis of nine laser-captured dopamine neuron and substantia nigra postmortem tissue investigations (Table 1) (15, 17–24). We used standardized processing of raw data from genome-wide expression studies, powerful analysis of biologically linked sets of genes, and

rigorous replication. To detect functionally important, coordinated changes in gene expression, we assessed multiple members of each biological pathway. We first applied a nonparametric rank-based method, Gene Set Enrichment Analysis (GSEA) (25, 26) which combines information from the members of biological pathways to increase the signal relative to noise. GSEA is advantageous compared to widely used parametric pathway analysis methods that are based on the hypergeometric test because no arbitrary cutoffs for enrichment are introduced (25, 27).

Combining the results of multiple independent studies increases the statistical power and precision of pathway associations when scarce human brain samples prohibit individual studies of large scale. Microarrays from multiple studies are sometimes considered to be part of one big study (the "pooling participants" method). Because unequal group sizes, in the presence of a lurking, confounding bias, can weight effect estimates incorrectly, results based on this method can be flawed or even outright paradoxical (Simpson's paradox) (28). A more objective strategy compares pathway associations with a phenotype within each genome-wide expression study (GWES) and then averages the estimates across multiple studies (29). Because GWESs typically differ vastly in sample size and in variance (a result of human biology, disease heterogeneity, and biospecimen processing), simply averaging effect estimates is not appropriate. A positive result in such a test can be due solely to bias rather than any relationship between pathway members and the phenotype of interest. It is important to weight averages to account for a data set's sample size and noise, instead of simply averaging associations from small and large, noisy, and high-quality data sets.

We overcame these challenges using random-effects model meta-analysis (termed meta-GSEA) and probed 522 gene sets for associations with PD across a total of 17 GWESs from 322 human brain and 88 blood samples in a three-stage design (nine, one, and seven GWESs included in stages 1, 2, and 3, respectively). This meta-analysis method uses weighted effect estimates that account for each data set's sample size and noise in order to estimate a summary effect for each gene set's association with PD.

RESULTS

Meta-analysis of 522 gene sets identifies molecular pathways associated with PD

We uniformly processed individual-level raw data (.CEL files), annotated probes to 522 curated biological processes, pathways, and gene sets (henceforth gene sets) predefined in the Broad Institute's Molecular Signatures Database (MSigDB) C2 v1.1 (25). MSigDB is a compilation of curated sets of genes that share common biological function or regulation based on evidence from pathway encyclopedias such as KEGG, BioCarta, GenMAPP; gene expression signatures systematically extracted from PubMed publications; and knowledge of domain experts. Using these gene sets and gene expression intensities, we tested for association of each of the 522 gene sets with PD in each of nine GWESs using GSEA (25), examined for study outliers, and then combined these results in a random-effects model meta-analysis across a total of 185 microarrays (99 from cases and 86 from controls) (stage 1 analysis; Table 1). One outlier data set was observed (fig. S1) but was conservatively included in the primary meta-analysis according to our intention to exclude gene sets solely based on study entry criteria [removal of the outlier data set further increased the strength of the observed associations (table S1)]. To control for differences in dopamine neuron numbers in patients with PD and control individuals, we derived three of the nine GWESs from dopamine neurons laser-captured from the substantia nigra of patients and control individuals. One of these GWESs is first presented here (Middleton-1) and one was unpublished at the time of analysis (NBD). In GSEA, for a given pair wise comparison, genes are ranked according to the difference in expression, and a nonparametric Kolmogorov-Smirnov statistic is applied to determine whether the rank ordering is random

or associated with the disease phenotype (25). Association of a gene set with the disease phenotype is quantified by normalized enrichment scores (NESs), with the sign of the NES indicating positive (overexpression) or negative (underexpression) enrichment of a gene set (25).

We then introduced a random-effects model meta-analysis to combine effect estimates for each of the 522 gene sets across nine laser-captured microdissected dopamine neuron (DA) and substantia nigra studies, termed meta-GSEA. This meta-analysis uses weighted averages of a NES to account for a data set's sample size and noise in order to estimate a summary NES (sNES). sNESs and 95% confidence intervals were calculated on the basis of a random-effects model, which uses weights that incorporate both within-study and between-study variance (30). The genome-wide significance threshold was conservatively specified as $P < 9.6 \times 10^{-5}$ (0.05 divided by 522, the number of gene sets tested). This Bonferroni correction is likely overly restrictive, because several gene sets are partially overlapping and therefore not truly independent tests. Twenty-eight gene sets with P values of $<9.6 \times 10^{-5}$ (range, $<10^{-8}$ to 0.00008) met our significance threshold (Fig. 1A and table S2). Key pathways were enriched across GWESs from substantia nigra homogenates (Zhang, Papapetropoulos, Moran, Miller, Hauser, and Grünblatt in Figs. 2 and 3, A and D) and GWESs derived from dopamine neurons laser-captured from substantia nigra [DA; data sets NBD and Middleton-1 in Figs. 2, 3, A and D, and 4A; the third DA data set (Cantuti) is a technical outlier (see fig. S1)]. Because we examined individual neurons in the DA data sets, these results cannot be explained by differences in proportions of dopamine neurons or glia assayed in the tissue.

We next examined the stability of these results (fig. S2). We iteratively left one study out at a time, performed meta-GSEA for the remaining eight studies, and scored the number of times 1 of the 28 gene sets achieved genome-wide significance in the left-in studies. Stability was 100% ($P < 9.6 \times 10^{-5}$ in each of nine unique iterations) for 19 gene sets. Thus, the meta-analysis results for 19 of 28 gene sets were highly stable and unaffected by removal of an individual study from the meta-analysis, whereas the results for the remaining gene sets were less stable.

Validation of 12 pathways in early subclinical disease

We selected gene sets for validation conservatively on the basis of the statistical evidence for association in stage 1. Unstable gene sets were included according to our intention to forward gene sets based on the genome-wide level of evidence. To determine whether the 28 gene sets identified in stage 1 are already perturbed in incipient PD (31–36), we interrogated pathway changes in postmortem substantia nigra of 16 cases with subclinical, PD-related, α-synuclein–positive, incidental Lewy body disease (PD-LBN), and in 17 age-, sex-, and postmortem interval (PMI)–matched controls without PD-related lesions on autopsy and also free of neurologic disease (Table 1 and table S3).

The presence of α-synuclein immunoreactive inclusions in neuronal cytoplasm (Lewy bodies) is mandatory for the neuropathologic confirmation of the clinical diagnosis of classical PD (35). In the clinically recognizable motor phase of sporadic PD, most patients display bradykinesia and resting tremor. The preclinical phase of PD has been estimated to precede motor impairment by >5 years based on nigral neuropathology, striatal dopamine transporter imaging, and nonmotor clinical symptoms (37). It is expected for any slowly progressive, aging-dependent disease that not all individuals live to cross the threshold from a subclinical phase to the clinically symptomatic phase (36). Indeed, an estimated 5 to 10% of individuals without motor symptoms during life display typical α-synuclein–positive Lewy bodies and neurites (36, 38), a reduction of dopamine markers (32–34), and mild and select loss of ventrolateral substantia nigra neurons on autopsy (35, 39). This had led to the

concept that brainstem α-synucleinopathy represents probable early, subclinical PD (32, 33, 35, 36, 39–41), although this is not without controversy (40, 42). In individuals with incidental Lewy body disease, the distribution of Lewy body inclusion is similar to that in PD (34, 36, 41, 43). The mild loss of substantia nigra neurons found in these individuals follows the regional pattern of cell loss seen in PD (predominant loss of the ventrolateral tier of the substantia nigra), but not in normal aging (predominant loss of the dorsolateral tier, with the ventrolateral tier being unaffected) (35, 39), This mild loss is associated with decreased striatal tyrosine hydroxylase (TH) (32–34) and vesicular monoamine transporter 2 immunoreactivity (33) that is intermediate to that seen in patients with late-stage PD and in healthy controls. As in overt PD, biochemical markers of oxidative stress are also increased in persons with incidental Lewy body disease (44, 45). Importantly, these individuals have not been treated with dopamine replacement therapy, thereby excluding PD medications as a confounding factor in the gene set analysis.

Twelve of the 28 gene sets were significantly associated with subclinical, mild, PD-related Lewy body neuropathology (36, 41), with *P* values of <0.05 (Table 2 and Fig. 3, B and E), suggesting that changes in these pathways reflect early pathobiological processes that may be prime targets for disease-modifying therapeutics.

Ten pathways are replicated in all three stages of analysis

In PD, α-synuclein immunoreactive Lewy bodies and Lewy neurites are present in a diversity of neurons outside the substantia nigra (36), and molecular or biochemical changes can be found in peripheral neuronal and even nonneuronal cells of patients with PD (46, 47) [and references in (13)]. Together with work in yeast and animal model systems (48), these data may indicate that dopamine neuron degeneration in PD is the result of general cellular defects to which dopamine neurons are simply more sensitive than other cells. To evaluate this hypothesis, we took the 12 gene sets forward for further evaluation in a total of 192 nonnigral samples (106 from cases, 86 from controls without neurodegenerative disease) from seven additional GWESs (Table 1). These include brain regions that show abundant Lewy body pathology without neuron loss in PD, such as frontal cortex (FC) and prefrontal cortex Broadman area 9 (BA9), as well as basal ganglia structures that are affected by biochemical changes in PD such as globus pallidus (GP) and putamen (PU). Additionally, one data set from human lymphoblastoid (LB) cell lines and one from whole cellular blood were included, because defects in mitochondrial function (46) and dopamine signaling (47) have been reported in peripheral blood cells in early untreated PD. These data sets represent, to our knowledge, all nonnigral GWESs in sporadic PD available at the time of analysis. Ten of the 12 gene sets had a *P* value of <0.05 in the raw data level meta-analysis of stage 3 with association in the same direction as the original signal (Table 2).

Overall, 10 of 12 gene sets analyzed in all stages showed a significant association in the same direction at each stage (Table 2). Ten gene sets reached a compelling degree of significance for association with PD in all three stages (*P* values better than 9.6×10^{-5} in stage 1, and better than 0.05 in stages 2 and 3), with *P* values below 10^{-5} in both the combined meta-analyses of substantia nigra stages 1 + 2 and stages 1 to 3 (Table 2).

Pathway analysis shows pervasive, coordinated defects in cellular energetics

The strongest statistical evidence for an association signal was for the electron transport chain (ETC) gene set (Table 2), one of a cluster of overlapping gene sets showing association in the stage 1 meta-analysis (-1.583, $<1 \times 10^{-8}$; Figs. 2 and 3A) and across stage 2 (-1.496, 1.46×10^{-2}; Fig. 3B) and stage 3 samples (-1.42, 1.66×10^{-5}; Fig. 3C). The ETC group contains 95 genes that include all subunits of the mitochondrial respiratory chain complexes I to V encoded by the nuclear human genome (13 subunits are encoded by

the mitochondrial genome). These were coordinately underexpressed in PD in laser-captured dopamine neurons (Figs. 3A and 4A), in subclinical PD-related Lewy body pathology (Fig. 4, C and D), and in the meta-analysis of nonnigral neuronal and blood cells (Fig. 3C). Overall, the estimate of effect was based on 410 microarrays (221 from cases and 189 from controls). In the NBD laser-captured dopamine neuron data set, the deficit in ETC gene set expression reached $P = 0.002$ (Fig. 3A), suggesting that the deficit in ETC expression in PD can be detected specifically in dopamine neurons of the substantita nigra. Underscoring the robustness of the association between PD and the ETC pathway, three other gene sets that in part contain constituents of the ETC were also significantly associated with PD (Fig. 1B; termed MAP00190 oxidative phosphorylation, VOXPHOS, and GO 0005739, respectively). These results (Table 2) indicate that our screen captured the pervasive changes in nuclear-encoded ETC to saturation and underscore the robustness of this observation.

The second strongest signal for a unique gene set was for the pyruvate metabolism gene set. The pyruvate metabolism gene set (Table 2) was underexpressed in stage 1 (-1.529, $P = 3.36 \times 10^{-8}$) and stage 2 (-1.844, $P = 2.37 \times 10^{-2}$), and to a lesser degree in nonnigral stage 3 (-1.062, $P = 4.59 \times 10^{-3}$). This association was also revealed by the biochemically linked and overlapping Krebs-TCA gene set (Table 2 and Fig. 1B). Together, the two gene sets encode the molecular machinery controlling entry of pyruvate, the intermediary resulting from glycolysis, into the Krebs cycle. Consistent with these molecular results in early-stage disease and with the abnormal glucose utilization seen in living patients (49, 50), the carbohydrate-responsive element–binding protein (ChREBP) pathway was also significantly underexpressed across all three stages of analysis (Table 2). The genes in the ChREBP pathway are distinct from the other gene sets identified (no gene overlap; Fig. 1B). ChREBP is a glucose-sensing transcription factor that transactivates key genes of glucose metabolism.

PGC-1α– responsive nuclear-encoded mitochondrial genes are underexpressed in PD

The transcriptional coactivator *PPARGC1A* (*PGC-1α*) is a master regulator of mitochondrial biogenesis and oxidative metabolism (51). In *PGC-1α* knockout mice, expression of genes responsible for mitochondrial respiration is markedly blunted, and mitochondrial enzymatic activities and concentrations of adenosine triphosphate (ATP) are decreased (52). Underexpression of a gene set of 425 *PGC-1α*–responsive genes (PGC) was significantly associated with PD pathology in the stage 1 meta-analysis (-1.366; $P = 6.75 \times 10^{-6}$; Fig. 3D), as well as with subclinical, mild, PD-related Lewy body neuropathology (36, 41) in stage 2 (-1.576; $P = 0.0496$; Fig. 3E), and across stage 3 samples (-0.884; $P = 0.0165$; Fig. 3F) (Table 2). Again, underexpression of the *PGC-1α*–responsive genes was clearly detectable in GWES of laser-captured dopamine neurons from PD cases compared with controls (Figs. 3D and 4A) and thus was not due to simple differences in proportions of dopamine neurons or glia in the specimens. *PGC-1α*–responsive genes were also underexpressed in substantia nigra of subclinical PD-related Lewy body neuropathology (36, 41) (Fig. 4, C and D). Thirty-one ETC genes are *PGC-1α*–responsive and thus are annotated both to the 95-gene ETC and the 425-gene PGC pathway. Even after omitting all 31 *PGC-1α*–responsive ETC genes from the PGC gene set, PGC was still robustly associated with PD (NES = -1.27, $P = 6.59 \times 10^{-5}$; -1.60, $P = 0.05$; and -0.8, $P = 0.036$, respectively, for the three stages). This indicates that *PGC-1α*–responsive genes other than those controlling ETC that are involved in mitochondrial protein import, mitochondrial protein folding, and mitochondrial translation were contributing to these association signals. Consistently, two additional gene sets that encode mitochondrial biogenesis genes, termed "mitochondr" and "human mitoDB 2002" (Fig. 1B; 108 of 447 and 111 of 428 genes, respectively, overlap with the PGC gene set), were associated with PD in all three analysis stages (Table 2). Collectively, this evidence indicates that *PGC-1α*–responsive genes are perturbed in PD and implicates *PGC-1α*–controlled ETC and *PGC1α*–controlled

mitochondrial bioenergetics defects in early and advanced molecular pathology in the substantia nigra, as well as in nonnigral tissues.

To confirm the underexpression of ETC and *PGC-1α*–responsive genes on a third gene expression platform in addition to the Illumina HumanHT-12v3 bead arrays (stage 2) and Affymetrix solid-phase arrays used in stages 1 and 3, we performed quantitative real-time polymerase chain reaction (qPCR) based on precise 5′ nuclease chemistry for 19 nuclear-encoded ETC genes selected on the basis of the microarray results (including 10 *PGC-1α*–responsive genes). Underexpression of these subsets of ETC and *PGC-1α*–responsive ETC genes was independently confirmed by qPCR in substantia nigra samples of a new population of 13 patients with PD and 17 age-, sex-, and PMI-matched controls without neurodegenerative disease, with $P = 3.8 \times 10^{-6}$ and $P = 0.002$, respectively, by a binomial test (Fig. 4B). Next, underexpression of the ETC and *PGC-1α*–responsive ETC genes was replicated by qPCR in 15 individuals with incidental Lewy body pathology and 17 age-, sex-, and PMI-matched control subjects used in stage 2, with $P = 3.8 \times 10^{-6}$ and $P = 0.002$, respectively, by a binomial test (Fig. 4D). These two qPCR studies confirmed the pathway changes measured by GWESs.

*PGC-1*α overexpression suppresses dopaminergic neuron loss induced by A53T–α-synuclein and rotenone

PGC-1α regulates a fundamental transcriptional cycle that modulates mitochondrial function and provides homeostatic control of cellular ATP (53). We investigated whether overexpression of *PGC-1α* coactivates transcription of nuclear-encoded electron transport genes and genetically blocks α-synuclein toxicity in a well-established cellular model of α-synucleinopathy (54–57). The model consists of primary cultures prepared from the midbrain region of E17 (embryonic day 17) rats. Transduction of the cells with adenovirus encoding α-synuclein that carries a human PD-linked mutation (A53T) results in a general loss of neurons, as manifested by a decrease in the number of cells that stain positive for the general neuronal marker MAP2 (56, 57). Dopaminergic (TH-positive) neurons are more vulnerable to the toxic effects of A53T overexpression than other neurons (for example, GABAergic neurons) in the cultures (55, 56). Therefore, with the primary midbrain cell culture model, one can monitor the preferential toxicity of α-synuclein to dopaminergic neurons relative to other neurons (and this preferential toxicity is thought to be relevant to PD pathogenesis). We found that cotransduction with adenovirus carrying human *PGC-1α* (but not the control *LacZ* gene) activated the expression of endogenous genes encoding nuclear subunits of the mitochondrial respiratory chain complexes I, II, IV, and V in neurons overexpressing A53T–α-synuclein (Fig. 5A). Moreover, the loss of TH-positive neurons induced by A53T–α-synuclein was rescued by cotransduction with adenovirus encoding human *PGC-1α* ($P < 0.01$; Fig. 5B). Furthermore, *PGC-1α* overexpression abrogated the A53T–α-synuclein–mediated retraction of MAP2- and TH-positive neuronal processes (Fig. 5C). These results indicate that expression of *PGC-1α* can up-regulate nuclear-encoded subunits of the mitochondrial respiratory chain and alleviate α-synuclein neurotoxicity in the primary midbrain culture model.

PD is a complex disease with strong environmental risk factors including exposure to pesticides (2) such as rotenone (1). Rotenone inhibits the transfer of electrons from iron-sulfur centers in complex I of the ETC to ubiquinone. Chronic systemic complex I inhibition caused by rotenone exposure induces features of PD in rats, including nigrostriatal dopaminergic degeneration and formation of α-synuclein–positive inclusions (5). The underlying mechanisms of rotenone-induced neuronal toxicity can be evaluated in in vitro models based on treating catecholaminergic neuronal cells with rotenone (3, 4). We investigated whether overexpression of *PGC-1α* can ameliorate rotenone toxicity in rat primary dopamine neurons and in human catecholaminergic SH-SY5Y neuronal cells, a

standard cellular system for modeling the biology of human substantia nigra dopamine neurons (16). The preferential loss of TH-positive neurons induced by exposure to rotenone was rescued by cotransduction with adenovirus encoding human *PGC-1α* ($P < 0.01$; Fig. 6A) in primary mesencephalic cultures. Overexpression of *PGC-1α* compared to the control gene *LacZ* coactivated the expression of nuclear-encoded subunits of complex I, II, III, IV, and V of the mitochondrial ETC (Fig. 6B) and induced a small but statistically significant increase in viability of human catecholaminergic SH-SY5Y cells exposed to rotenone (14% increase; $P = 0.02$; Fig. 6C). The MTT assay, which measures the reduction of 3-(4,5-dimethylthiazol-2-yl)-2,5-diphenyl tetrazolium bromide into formazan by cellular and mitochondrial dehydrogenases (58), was used to estimate cell viability.

Another neurotoxin, 1-methyl-4-phenyl-1,2,3,6-tetrahydropyridine (MPTP), causes selective death of dopaminergic neurons in the substantia nigra pars compacta (SNpc) and parkinsonism in humans, and is widely used to model PD in rodents and primates (6, 59). Consistent with our human and in vitro data, St-Pierre and colleagues provided evidence in mice that genetic ablation of the *PGC-1α* gene markedly enhances MPTP-induced loss of TH-positive neurons in the substantia nigra (60). MPTP exposure caused a 61% loss of TH-positive neurons in the substantia nigra of *PGC-1α* knockout mice but only a 12% loss in wild-type mice (60).

By integrating a large-scale gene expression database and genome-wide pathway analysis with validation in subclinical disease and mechanistic analysis in primary dopaminergic neurons, we found that nuclear-encoded *PGC-1α*–responsive bioenergetics and ETC genes are coordinately underexpressed in human PD and in incipient Lewy body disease, and that *PGC-1α* coactivates these genes and blocks A53T–α-synuclein– and rotenone-induced dopamine neuron loss in cellular disease models.

DISCUSSION

Here, we have conducted a comprehensive assessment of currently available data on gene expression in PD, integrating 17 studies and 14 million data points of 322 human brain and 88 blood samples. To identify molecular pathways associated with PD, we combined genome-wide expression analysis of human laser-captured dopamine neurons and substantia nigra postmortem tissue from PD patients, large-scale pathway meta-analysis, and validation on multiple platforms, as well as evaluation of individuals likely to be in the earliest stages of Lewy body disease. Our study found that decreases in expression of 10 gene sets are associated with PD, even in probable subclinical disease and in tissues outside the substantia nigra. These 10 gene sets encode proteins responsible for four distinct, but interconnected, cellular processes: nuclear-encoded mitochondrial electron transport, mitochondrial biogenesis, glucose utilization, and glucose sensing. We show that bioenergetics genes responsive to the master regulator *PGC-1α*, including nuclear-encoded ETC genes, are underexpressed in patients with PD and in incipient Lewy body disease. In addition, coactivation by *PGC-1α* up-regulates nuclear subunits of mitochondrial respiratory chain complexes I, II, III, IV, and V and blocks dopamine neuron loss in cellular models of PD-linked α-synucleinopathy and rotenone toxicity. Consistent with a mechanistic role in the onset of the human disease proposed by our observations, genetic ablation of *PGC-1α* in mice markedly enhances MPTP-induced dopamine neuron loss in the substantia nigra (60). This neurotoxin is widely used to model PD in primates and rodents (61) and caused a 61% loss of TH-positive neurons in the substantia nigra of *PGC-1α* knockout mice but only a 12% loss in wild-type mice (60).

Physiology, pharmacology, and clinical and genetic investigation support the relationship between PD and the two main components required for energy metabolism in neurons:

electron transport carriers and glucose utilization. For example, the ability of complex I to transfer electrons from NADH to ubiquinone (coenzyme Q) was impaired in mitochondria purified from the FC of five individuals with PD (62), and complex III and IV activity was also reduced, although to a lower extent (62). Complex I subunits in FC specimens from 10 patients with PD exhibited increased protein carbonyl content, indicating oxidative damage, and this inversely correlated to rates of NADH-driven electron flow in the tissue (63). ETC dysfunction is also found in platelets from patients with PD, defective oxidative phosphorylation may occur in muscle, and the oxidative stress marker 8-hydroxydeoxyguanosine is elevated in plasma of patients with PD (7). Complex I inhibitors such as MPTP and rotenone cause dopamine cell death and parkinsonism (7). Nevertheless, the precise contribution of complex I dysfunction in the etiology of common, sporadic PD has remained unclear (64). Genetically, mutations in the mitochondrially targeted serine-threonine kinase PTEN-induced putative kinase-1 (*PINK1)* and the E3 ubiquitin ligase Parkin (*PARK2*) cause autosomal recessive PD in rare families. Mutations in *PARK2* and *PINK1* lead to mitochondrial swelling in fruit flies (8, 9) and involve a pathway that links ubiquitylation with selective autophagy of damaged mitochondria (65). A relationship between glucose utilization and PD is supported in living patients. Magnetic resonance spectroscopy (49) and 2-[^{18}F]fluoro-2-deoxy-D-glucose PET studies (50) demonstrate increased lactate concentrations and glucose hypometabolism, consistent with a general shift to anaerobic glycolysis in the neocortex of PD patients.

On the basis of our data presented here, we hypothesize that PD is characterized by pervasive, coordinated, nuclear-encoded cellular energetic defects to which nigral dopamine neurons are intrinsically more susceptible than other cells. Complex I deficiency in PD may be a biochemically detectable "tip of the iceberg" of a deeper molecular defect comprising the entire nuclear-encoded ETC. Underexpression of *PGC-1α*–controlled genes involved in cellular energetics might represent a common link for these diverse manifestations of defects in mitochondrial biogenesis and energetics, and abnormal glucose utilization. If this hypothesis is valid, it would suggest that modulation of cellular energetics could be used to prevent or treat PD, and that monitoring cellular energetics could serve as a diagnostic tool.

The results of this study should be interpreted bearing in mind its limitations. First, although every effort was made to ascertain all appropriate publications, it is possible that some were missed. Second, undetected publication bias, which could arise from the underreporting of studies that show a negative finding, may confound the results of a meta-analysis. However, several provisions in this study make this unlikely. We identified and included five unpublished GWES data sets. We were the first to analyze pathway enrichment by using GSEA in each of the studies (in other words, all individual GSEA results are new and thus did not directly influence publication decisions). In addition, we examined the effect of leaving out the first as well as any other nigral GWES study published on the effect estimates (none found on replicated gene sets; fig. S2). Third, the number and quality of annotated gene sets is evolving. The gene sets evaluated in this study likely represent only a subset of all true biological pathways or processes and are subject to updates as biomedical knowledge increases. Because pathway encyclopedias are systematically expanded, this PD gene expression database will be a useful resource for testing new gene sets for association with human PD. Fourth, the staged approach used is designed to yield true-positive results by extensively validating candidate pathways identified in stage 1. It is, however, prone to false negatives because only gene sets robustly associated with late-stage disease are forwarded for replication in subjects with incipient pathology. This tiered approach cannot detect gene sets exclusively associated with initial, but not late-stage, pathology. Larger sample sizes of high-quality incidental Lewy body cases will be needed to systematically identify all molecular pathways associated with early pathology. Fifth, expression analysis of postmortem substantia nigra alone cannot distinguish between associations reflecting the

molecular pathobiology of PD versus proliferation of glia or depletion of dopamine neurons in patient tissue. To correct for this bias, we used laser-capture of dopamine neurons. In an analysis of individual dopamine neurons, both ETC and PGC pathways were strongly underexpressed. In our study, pathway associations were further evaluated in subclinical PD-related Lewy body disease (36, 41), in which there is only mild loss of dopamine neurons (35, 39), as well as in brain regions and blood cells that show histopathological or biochemical changes in PD, but not cell loss. Collectively then, analysis of laser-captured dopamine neuron data sets, recapitulation in early disease, and tissues not subject to neuron loss in PD indicate that the pathways here associated with PD are not materially confounded by glial proliferation or depletion of dopamine neurons.

Methods like the meta-GSEA approach we have used here will be useful for identifying disease-linked pathway signals in other diseases by integrating measurements of multiple genes and multiple genome-wide expression studies. This may be necessary when the molecular processes leading to common complex diseases result from modest variation in the expression of multiple members of a pathway, when both environmental and genetic contributions are integrated in the pathway signature, or when access to biospecimens is limited.

METHODS

Bioinformatics and biostatistics methods

The coordinating principal investigator of a Michael J. Fox Foundation genetics consortium award invited the corresponding authors of genome-wide expression studies in PD published in the English language and representing eight or more arrays to serve as collaborating investigators of the Global PD Gene Expression Consortium and to contribute unprocessed raw data (for example, CEL files) underlying their published work as well as unpublished data. These publications were identified via PubMed and Gene Expression Ominbus (GEO) searches by using the terms "Parkinson's disease" and "gene expression" or "transcriptional profiling," as of January 31, 2008. The collaborating investigators were asked to contribute clinical and raw genome-wide expression data to the bioinformatics core. In total, 17 microarray data sets (Table 1) were analyzed: 11 data sets were identified through PubMed (15, 17–23), 1 through the National Brain Databank, 4 new data sets were contributed by co-investigators, and 1 was generated for the stage 2 replication study. Eleven of 17 studies were previously published (15, 17–23), 5 are newly published in the current study, 1 was unpublished at the start of our analysis, but has since been published elsewhere (24). Affymetrix. CEL files from all data set were normalized to "all probe sets" in a standardized matter and scaled to 100 by the MAS5 algorithm implemented in the Bioconductor package (66).

Gene Set Enrichment Analysis

GSEA is a nonparametric method (25, 26) to determine whether a pre-defined gene set is enriched at the top or bottom of a list of all genes assayed rank-ordered by their association with the phenotype (using an appropriate metric, generally signal-to-noise ratio). GSEA was performed for each of the 17 data sets as described (25, 26) (see also Supplementary Material). For each gene set, an enrichment score was calculated, which is a normalized Kolmogorov-Smirnov statistic. To adjust for different sizes of gene sets, a positive (negative) normalized enrichment score (NES) was computed (25, 26).

Meta-GSEA

Meta-analysis provides a means to quantitatively combine results from several studies on a specific topic. We used the NES as estimate of effect size and combined these estimates

across studies by adapting a random-effects model meta-analysis statistic that accounts for both study variance and between-study variance (30). Results of a fixed-effect meta-analysis strictly apply to the studies involved in the given meta-analysis, whereas random effect model estimates such as we used here are intended to make inferences to a superpopulation of studies from which those actually analyzed were randomly or at least representatively selected.

The random-effects model summary effect-size estimate of a gene set ($\overline{T}_{.}^{*}$) - the sNES - is calculated as follows:

$$\overline{T}_{.}^{*} = \frac{\sum_{i=1}^{k} w_i^* T_i}{\sum_{i=1}^{k} w_i^*}$$

(1)

where T_i is the NES in the ith data set and w_i^* is an estimated optimal weight that is the reciprocal of the variance and given by:

$$w_i^* = \frac{1}{v_i^*} = \frac{1}{v_i + \widehat{\tau^2}}$$

(2)

where v_i is calculated from a bootstrap procedure as described below, and $\widehat{\tau^2}$ is the estimated between-study variance component. $\widehat{\tau^2}$ is estimated by Eqs. 3 to 6:

$$\widehat{\tau^2} = \begin{cases} \frac{Q-(k-1)}{c} & if \quad Q \geq k-1 \\ 0 & if \quad Q < k-1 \end{cases}$$

(3)

$$c = \sum_{i=1}^{k} w_i - \frac{\sum_{i=1}^{k} (w_i)^2}{\sum_{i=1}^{k} w_i}$$

(4)

$$Q = \sum_{i=1}^{k} w_i (T_i - \overline{T}.)^2$$

(5)

$$\overline{T}. = \frac{\sum_{i=1}^{k} w_i T_i}{\sum_{i=1}^{k} w_i}$$

(6)

where $\bar{T}$ is the weighted mean of NESs for one gene set, w_i is reciprocal of v_i and k is the total number of studies.

The variance of the random-effects $\bar{T}^*$ is given by the reciprocal of the sum of the random-effects weights:

$$v_{.}^* = \frac{1}{\sum_{i=1}^{k} w_i^*}$$

(7)

The 95% Confidence interval (CI) for the mean effect μ is calculated by:

$$\bar{T}_{.}^* - z_{\alpha/2}\sqrt{v_{.}^*} \le \mu \le \bar{T}_{.}^* + z_{\alpha/2}\sqrt{v_{.}^*}$$

(8)

where $z_{\alpha/2}$ is the two-tailed critical region of the standard normal distribution; for $\alpha = 0.05$ and 95% confidence intervals, $z_{\alpha/2} = 1.96$.

Bootstrap procedure

For each data set, we bootstrapped case and control samples separately and recomputed the NES of a gene set for each iteration. This procedure was repeated 5000 times. Because the distribution of the 5000 bootstrapped samples was bimodal, we randomly selected 1000 positive (or negative) NES from the 5000 bootstrap samples if the observed NES was positive (or negative) (25). The variance of a gene set was estimated as the observed variance of the bootstrap-generated frequency distribution of the 1000 NESs.

Estimating the significance of a sNES

We used a permutation procedure to generate a random null distribution of a sNES for a gene set. First, we generated two 522×9 matrices: one containing the NES and one containing the weights for the 522 gene sets and 9 nigral data sets. Then we randomly but concordantly permuted the two matrices so that, at each permutation, a weight was always yoked to its corresponding NES. A sNES was recomputed by the meta-analysis method described above. This procedure was repeated 100 million times. The *P* value for an observed sNES was the proportion of sNES in the permutation-generated frequency distribution that exceeded the observed sNES in absolute value. The same procedure was applied for the meta-GSEAs across stage 3, as well as across the 17 microarray data sets, and across 10 substantia nigra microarray data sets, respectively.

Laboratory methods: Brain samples

For the PD-LBN GWES (Table 1 and table S3), substantia nigra tissue was obtained from snap-frozen human substantia nigras of 16 individuals with a clinicopathological diagnosis of incidental Lewy body disease. These individuals had incidental Lewy body pathology on neuropathologic examination, with Lewy bodies detected in some cases in the olfactory bulb only, or in brainstem nuclei of locus coeruleus and substantia nigra only, but not in the neocortex, consistent with early stage PD. Seventeen age-, sex-, PMI-, and RNA integrity number–matched controls, who were clinicopathologically within normal limits for age (see Table 1 and table S3 for detail), were included. Human brain samples used for the stage 2 GWES, as well for the two qPCR validation studies (Fig. 4, B and 4D), were collected under the Brain and Body Donation Program at Sun Health Research Institute or obtained from the Harvard Brain Tissue Resource Center at McLean Hospital and the Massachusetts

Alzheimer Disease Research Center Tissue Resource Center. All protocols were approved by the Institutional Review Board of Brigham and Women's Hospital.

Brain samples used for Middleton-1, Middleton-2, and Miller GWES, as well as human LB cell lines used for Middleton-3 are described in Table 1 and Supplementary Material.

Laser microdissection of SN pars compacta neurons

To quantify expression changes in individual SN pars compacta (pc) neurons proper in the Middleton-1 GWES (Table 1 and Fig. 2), we used a laser microdissection instrument (AS-LMD, Leica) to isolate SNpc cells for RNA isolation. Control and PD subjects were matched for age and PMI. Multiple 16-μm sections of midbrain from each subject were obtained on a cryostat at −20°C and mounted on the membrane of PEN (polyethylene naphthalate) foil slides (Leica). Adjacent slides were taken and stained for cytoarchitectural visualization (Nissl staining) of the SNpc. A total of about 80 to 200 darkly pigmented neurons were obtained from the SNpc in five to eight sections from each subject. These cells were readily visualized in the unstained frozen sections, where they were manually outlined with a computer mouse at x200 magnification using the LMD 6000 AVC software (Leica). After outlining, the LMD apparatus automatically dissected the identified cells free of the PEN foil slide using a highly focused laser beam that followed the outlined path and allowed the cells to fall into a PCR tube cap containing 30 μl of RLT Lysis Buffer from the RNeasy Mini Kit (Qiagen). To maximize RNA integrity, we obtained all of the cells of interest from each frozen section within 10 min.

Genome-wide expression studies

For the PD-LBN GWES of incidental Lewy body cases and controls (stage 2; Table 1), RNA was isolated and quality-controlled by Agilent Bioanalyzer as described (16). Only RNAs with preserved ribosomal peaks on electropherogram were forwarded for analysis, and RNA integrity numbers of cases and controls were matched. Total RNA (350 ng) was reverse-transcribed from each substantia nigra sample and hybridized to Illumina HumanHT-12v3 Expression BeadChips targeting more than 25,000 annotated genes with 48,803 probes derived from the National Center for Biotechnology Information (NCBI) Reference Sequence RefSeq (Build 36.2, Rel 22) and the UniGene (Build 99) databases, and scanned on a BeadArray Reader. Data were processed, normalized by "average normalization," and quality-controlled with GenomeStudio. Procedures for the Middleton-1, Middleton-2, Middleton-3, and Miller GWES are described in the Supplementary Material.

All 17 GWES data sets have been submitted to publicly available databases under GEO accession numbers GSE6613, GSE7621, GSE8397 (two data sets), GSE20141, GSE20146, GSE20153, GSE20159, GSE20163, GSE20164, GSE20168, GSE20291, GSE20292, GSE20314, GSE20333, and GSE24378; and National Brain Databank accession name "Parkinson's."

Quantitative PCR experiments were performed similarly as in (16) and are reported in the Supplementary Material.

Cell culture experiments

Methods for experiments involving cellular models of A53T–α-synuclein-toxicity (54–57) and rotenone toxicity are reported in the Supplementary Material.

Supplementary Material

Refer to Web version on PubMed Central for supplementary material.

Acknowledgments

REFERENCES AND NOTES

1. Dhillon AS, Tarbutton GL, Levin JL, Plotkin GM, Lowry LK, Nalbone JT, Shepherd S. Pesticide/ environmental exposures and Parkinson's disease in East Texas. J Agromedicine. 2008; 13:37. [PubMed: 19042691]

2. Chade AR, Kasten M, Tanner CM. Nongenetic causes of Parkinson's disease. J Neural Transm. 2006; (Suppl):147.

3. Sherer TB, Betarbet R, Testa CM, Seo BB, Richardson JR, Kim JH, Miller GW, Yagi T, Matsuno-Yagi A, Greenamyre JT. Mechanism of toxicity in rotenone models of Parkinson's disease. J Neurosci. Nov 26.2003 23:10756. [PubMed: 14645467]

4. Park HJ, Kim HJ, Park HK, Chung JH. Protective effect of histamine H2 receptor antagonist ranitidine against rotenone-induced apoptosis. Neurotoxicology. Nov.2009 30:1114. [PubMed: 19723537]

5. Betarbet R, Sherer TB, MacKenzie G, Garcia-Osuna M, Panov AV, Greenamyre JT. Chronic systemic pesticide exposure reproduces features of Parkinson's disease. Nat Neurosci. Dec.2000 3:1301. [PubMed: 11100151]

6. Langston JW, Ballard P, Tetrud JW, Irwin I. Chronic Parkinsonism in humans due to a product of meperidine-analog synthesis. Science. Feb 25.1983 219:979. [PubMed: 6823561]

7. Henchcliffe C, Beal MF. Mitochondrial biology and oxidative stress in Parkinson disease pathogenesis. Nat Clin Pract Neurol. Nov.2008 4:600. [PubMed: 18978800]

8. Park J, Lee SB, Lee S, Kim Y, Song S, Kim S, Bae E, Kim J, Shong M, Kim JM, Chung J. Mitochondrial dysfunction in Drosophila PINK1 mutants is complemented by parkin. Nature. Jun 29.2006 441:1157. [PubMed: 16672980]

9. Greene JC, Whitworth AJ, Kuo I, Andrews LA, Feany MB, Pallanck LJ. Mitochondrial pathology and apoptotic muscle degeneration in Drosophila parkin mutants. Proc Natl Acad Sci U S A. Apr 1.2003 100:4078. [PubMed: 12642658]

10. Devi L, Raghavendran V, Prabhu BM, Avadhani NG, Anandatheerthavarada HK. Mitochondrial import and accumulation of alpha-synuclein impair complex I in human dopaminergic neuronal cultures and Parkinson disease brain. J Biol Chem. Apr 4.2008 283:9089. [PubMed: 18245082]

11. Roy S, Wolman L. Ultrastructural observations in Parkinsonism. J Pathol. Sep.1969 99:39. [PubMed: 5359222]

12. Scherzer CR, Offe K, Gearing M, Rees HD, Fang G, Heilman CJ, Schaller C, Bujo H, Levey AI, Lah JJ. Loss of apolipoprotein E receptor LR11 in Alzheimer disease. Arch Neurol. Aug.2004 61:1200. [PubMed: 15313836]

13. Scherzer CR. Chipping away at diagnostics for neurodegenerative diseases. Neurobiol Dis. Mar 10.2009

14. Schadt EE, Lamb J, Yang X, Zhu J, Edwards S, Guhathakurta D, Sieberts SK, Monks S, Reitman M, Zhang C, Lum PY, Leonardson A, Thieringer R, Metzger JM, Yang L, Castle J, Zhu H, Kash SF, Drake TA, Sachs A, Lusis AJ. An integrative genomics approach to infer causal associations between gene expression and disease. Nat Genet. Jul.2005 37:710. [PubMed: 15965475]

15. Scherzer CR, Eklund AC, Morse LJ, Liao Z, Locascio JJ, Fefer D, Schwarzschild MA, Schlossmacher MG, Hauser MA, Vance JM, Sudarsky LR, Standaert DG, Growdon JH, Jensen RV, Gullans SR. Molecular markers of early Parkinson's disease based on gene expression in blood. Proc Natl Acad Sci U S A. Jan 16.2007 104:955. [PubMed: 17215369]

16. Scherzer CR, Grass JA, Liao Z, Pepivani I, Zheng B, Eklund AC, Ney PA, Ng J, McGoldrick M, Mollenhauer B, Bresnick EH, Schlossmacher MG. GATA transcription factors directly regulate the Parkinson's disease-linked gene alpha-synuclein. Proc Natl Acad Sci U S A. Aug 5.2008 105:10907. [PubMed: 18669654]

17. Grunblatt E, Mandel S, Jacob-Hirsch J, Zeligson S, Amariglo N, Rechavi G, Li J, Ravid R, Roggendorf W, Riederer P, Youdim MB. Gene expression profiling of parkinsonian substantia substantia nigra pars compacta; alterations in ubiquitin-proteasome, heat shock protein, iron and oxidative stress regulated proteins, cell adhesion/cellular matrix and vesicle trafficking genes. J Neural Transm. 2004; 111:1543–1573. [PubMed: 15455214]

18. Hauser MA, Li YJ, Xu H, Noureddine MA, Shao YS, Gullans SR, Scherzer CR, Jensen RV, McLaurin AC, Gibson JR, Scott BL, Jewett RM, Stenger JE, Schmechel DE, Hulette CM, Vance JM. Expression profiling of substantia nigra in Parkinson disease, progressive supranuclear palsy, and frontotemporal dementia with parkinsonism. Arch Neurol. 2005; 62:917–921. [PubMed: 15956162]

19. Moran LB, Duke DC, Deprez M, Dexter DT, Pearce RK, Graeber MB. Whole genome expression profiling of the medial and lateral substantia nigra in Parkinson's disease. Neurogenetics. 2006; 7:1–11. [PubMed: 16344956]

20. Papapetropoulos S, Ffrench-Mullen J, McCorquodale D, Qin Y, Pablo J, Mash DC. Multiregional gene expression profiling identifies MRPS6 as a possible candidate gene for Parkinson's disease. Gene Expr. 2006; 13:205–215. [PubMed: 17193926]

21. Cantuti-Castelvetri I, Keller-McGandy C, Bouzou B, Asteris G, Clark TW, Frosch MP, Standaert DG. Effects of gender on nigral gene expression and Parkinson disease. Neurobiol Dis. 2007; 26:606–614. [PubMed: 17412603]

22. Zhang Y, James M, Middleton FA, Davis RL. Transcriptional analysis of multiple brain regions in Parkinson's disease supports the involvement of specific protein processing, energy metabolism, and signaling pathways, and suggests novel disease mechanisms. Am J Med Genet B Neuropsychiatr Genet. 2005; 137B:5–16. [PubMed: 15965975]

23. Vogt IR, Lees AJ, Evert BO, Klockgether T, Bonin M, Wullner U. Transcriptional changes in multiple system atrophy and Parkinson's disease putamen. Exp Neurol. 2006; 199:465–478. [PubMed: 16626704]

24. Simunovic F, Yi M, Wang Y, Macey L, Brown LT, Krichevsky AM, Andersen SL, Stephens RM, Benes FM, Sonntag KC. Gene expression profiling of substantia nigra dopamine neurons: Further insights into Parkinson's disease pathology. Brain. 2009; 132:1795–1809. [PubMed: 19052140]

25. Subramanian A, Tamayo P, Mootha VK, Mukherjee S, Ebert BL, Gillette MA, Paulovich A, Pomeroy SL, Golub TR, Lander ES, Mesirov JP. Gene set enrichment analysis: a knowledge-based approach for interpreting genome-wide expression profiles. Proc Natl Acad Sci U S A. Oct 25.2005 102:15545. [PubMed: 16199517]

26. Subramanian A, Kuehn H, Gould J, Tamayo P, Mesirov JP. GSEA-P: a desktop application for Gene Set Enrichment Analysis. Bioinformatics. Dec 1.2007 23:3251. [PubMed: 17644558]

27. Mootha VK, Lindgren CM, Eriksson KF, Subramanian A, Sihag S, Lehar J, Puigserver P, Carlsson E, Ridderstrale M, Laurila E, Houstis N, Daly MJ, Patterson N, Mesirov JP, Golub TR, Tamayo P, Spiegelman B, Lander ES, Hirschhorn JN, Altshuler D, Groop LC. PGC-1alpha-responsive genes involved in oxidative phosphorylation are coordinately downregulated in human diabetes. Nat Genet. Jul.2003 34:267. [PubMed: 12808457]

28. Blyth CR. On Simpson's Paradox and the Sure-Thing Principle. Journal of the American Statistical Association. 1972; 67:364.

29. Thomassen M, Tan Q, Kruse TA. Gene expression meta-analysis identifies chromosomal regions and candidate genes involved in breast cancer metastasis. Breast Cancer Res Treat. Jan.2009 113:239. [PubMed: 18293085]

30. Hedges LV, Vevea JL. Fixed- and random-effects models in meta-analysis. Psychological Methods. 1998; 3:486.

31. Jellinger KA. A critical evaluation of current staging of alpha-synuclein pathology in Lewy body disorders. Biochim Biophys Acta. Jul.2009 1792:730. [PubMed: 18718530]

32. Dickson DW, Fujishiro H, DelleDonne A, Menke J, Ahmed Z, Klos KJ, Josephs KA, Frigerio R, Burnett M, Parisi JE, Ahlskog JE. Evidence that incidental Lewy body disease is pre-symptomatic Parkinson's disease. Acta Neuropathol. Apr.2008 115:437. [PubMed: 18264713]

33. DelleDonne A, Klos KJ, Fujishiro H, Ahmed Z, Parisi JE, Josephs KA, Frigerio R, Burnett M, Wszolek ZK, Uitti RJ, Ahlskog JE, Dickson DW. Incidental Lewy body disease and preclinical Parkinson disease. Arch Neurol. Aug.2008 65:1074. [PubMed: 18695057]

34. Beach TG, Adler CH, Sue LI, Peirce JB, Bachalakuri J, Dalsing-Hernandez JE, Lue LF, Caviness JN, Connor DJ, Sabbagh MN, Walker DG. Reduced striatal tyrosine hydroxylase in incidental Lewy body disease. Acta Neuropathol. Apr.2008 115:445. [PubMed: 17985144]

35. Fearnley JM, Lees AJ. Ageing and Parkinson's disease: substantia nigra regional selectivity. Brain. Oct.1991 114(Pt 5):2283. [PubMed: 1933245]

36. Braak H, Del Tredici K, Rub U, de Vos RA, Jansen Steur EN, Braak E. Staging of brain pathology related to sporadic Parkinson's disease. Neurobiol Aging. Mar-Apr.2003 24:197. [PubMed: 12498954]

37. Savica R, Rocca WA, Ahlskog JE. When does Parkinson disease start? Arch Neurol. Jul.67:798. [PubMed: 20625084]

38. Forno L. Concentric hyalin intraneuronal inclusions of Lewy type in the brains of elderly persons (50 incidental cases): relationship to parkinsonism. J Am Geriatr Soc. 1969; 17:557. [PubMed: 4182529]

39. Ross GW, Petrovitch H, Abbott RD, Nelson J, Markesbery W, Davis D, Hardman J, Launer L, Masaki K, Tanner CM, White LR. Parkinsonian signs and substantia nigra neuron density in decendents elders without PD. Ann Neurol. Oct.2004 56:532. [PubMed: 15389895]

40. Jellinger KA. Critical evaluation of the Braak staging scheme for Parkinson's disease. Ann Neurol. Apr.67:550. [PubMed: 20437592]

41. Braak H, Del Tredici K. Invited Article: Nervous system pathology in sporadic Parkinson disease. Neurology. May 13.2008 70:1916. [PubMed: 18474848]

42. Burke RE, Dauer WT, Vonsattel JP. A critical evaluation of the Braak staging scheme for Parkinson's disease. Ann Neurol. Nov.2008 64:485. [PubMed: 19067353]

43. Dickson DW, Uchikado H, Fujishiro H, Tsuboi Y. Evidence in favor of Braak staging of Parkinson's disease. Mov Disord. 25(Suppl 1):S78. [PubMed: 20187227]

44. Dalfo E, Portero-Otin M, Ayala V, Martinez A, Pamplona R, Ferrer I. Evidence of oxidative stress in the neocortex in incidental Lewy body disease. J Neuropathol Exp Neurol. Sep.2005 64:816. [PubMed: 16141792]

45. Dexter DT, Sian J, Rose S, Hindmarsh JG, Mann VM, Cooper JM, Wells FR, Daniel SE, Lees AJ, Schapira AH, et al. Indices of oxidative stress and mitochondrial function in individuals with incidental Lewy body disease. Ann Neurol. Jan.1994 35:38. [PubMed: 8285590]

46. Haas RH, Nasirian F, Nakano K, Ward D, Pay M, Hill R, Shults CW. Low platelet mitochondrial complex I and complex II/III activity in early untreated Parkinson's disease. Ann Neurol. Jun.1995 37:714. [PubMed: 7778844]

47. Barbanti P, Fabbrini G, Ricci A, Cerbo R, Bronzetti E, Caronti B, Calderaro C, Felici L, Stocchi F, Meco G, Amenta F, Lenzi GL. Increased expression of dopamine receptors on lymphocytes in Parkinson's disease. Mov Disord. Sep.1999 14:764. [PubMed: 10495037]

48. Scherzer CR, Feany MB. Yeast genetics targets lipids in Parkinson's disease. Trends Genet. Jul. 2004 20:273. [PubMed: 15219388]

49. Bowen BC, Block RE, Sanchez-Ramos J, Pattany PM, Lampman DA, Murdoch JB, Quencer RM. Proton MR spectroscopy of the brain in 14 patients with Parkinson disease. AJNR Am J Neuroradiol. Jan.1995 16:61. [PubMed: 7900603]

50. Hu MT, Taylor-Robinson SD, Chaudhuri KR, Bell JD, Labbe C, Cunningham VJ, Koepp MJ, Hammers A, Morris RG, Turjanski N, Brooks DJ. Cortical dysfunction in non-demented Parkinson's disease patients: a combined (31)P-MRS and (18)FDG-PET study. Brain. Feb.2000 123(Pt 2):340. [PubMed: 10648441]

51. Lin J, Handschin C, Spiegelman BM. Metabolic control through the PGC-1 family of transcription coactivators. Cell Metab. Jun.2005 1:361. [PubMed: 16054085]

52. Arany Z, He H, Lin J, Hoyer K, Handschin C, Toka O, Ahmad F, Matsui T, Chin S, Wu PH, Rybkin, Shelton JM, Manieri M, Cinti S, Schoen FJ, Bassel-Duby R, Rosenzweig A, Ingwall JS, Spiegelman BM. Transcriptional coactivator PGC-1 alpha controls the energy state and contractile function of cardiac muscle. Cell Metab. Apr.2005 1:259. [PubMed: 16054070]

53. Rohas LM, St-Pierre J, Uldry M, Jager S, Handschin C, Spiegelman BM. A fundamental system of cellular energy homeostasis regulated by PGC-1alpha. Proc Natl Acad Sci U S A. May 8.2007 104:7933. [PubMed: 17470778]

54. Cooper AA, Gitler AD, Cashikar A, Haynes CM, Hill KJ, Bhullar B, Liu K, Xu K, Strathearn KE, Liu F, Cao S, Caldwell KA, Caldwell GA, Marsischky G, Kolodner RD, Labaer J, Rochet JC, Bonini NM, Lindquist S. Alpha-synuclein blocks ER-Golgi traffic and Rab1 rescues neuron loss in Parkinson's models. Science. Jul 21.2006 313:324. [PubMed: 16794039]

55. Liu F, Nguyen JL, Hulleman JD, Li L, Rochet JC. Mechanisms of DJ-1 neuroprotection in a cellular model of Parkinson's disease. J Neurochem. Jun.2008 105:2435. [PubMed: 18331584]

56. Gitler AD, Chesi A, Geddie ML, Strathearn KE, Hamamichi S, Hill KJ, Caldwell KA, Caldwell GA, Cooper AA, Rochet JC, Lindquist S. Alpha-synuclein is part of a diverse and highly conserved interaction network that includes PARK9 and manganese toxicity. Nat Genet. Mar.2009 41:308. [PubMed: 19182805]

57. Liu F, Hindupur J, Nguyen JL, Ruf KJ, Zhu J, Schieler JL, Bonham CC, Wood KV, Davisson VJ, Rochet JC. Methionine sulfoxide reductase A protects dopaminergic cells from Parkinson's disease-related insults. Free Radic Biol Med. Aug 1.2008 45:242. [PubMed: 18456002]

58. Berridge MV, Tan AS. Characterization of the cellular reduction of 3-(4,5-dimethylthiazol-2-yl)-2,5-diphenyltetrazolium bromide (MTT): subcellular localization, substrate dependence, and involvement of mitochondrial electron transport in MTT reduction. Arch Biochem Biophys. Jun. 1993 303:474. [PubMed: 8390225]

59. Przedborski S, Tieu K, Perier C, Vila M. MPTP as a mitochondrial neurotoxic model of Parkinson's disease. J Bioenerg Biomembr. Aug.2004 36:375. [PubMed: 15377875]

60. St-Pierre J, Drori S, Uldry M, Silvaggi JM, Rhee J, Jager S, Handschin C, Zheng K, Lin J, Yang W, Simon DK, Bachoo R, Spiegelman BM. Suppression of reactive oxygen species and neurodegeneration by the PGC-1 transcriptional coactivators. Cell. Oct 20.2006 127:397. [PubMed: 17055439]

61. Silva RM, Ries V, Oo TF, Yarygina O, Jackson-Lewis V, Ryu EJ, Lu PD, Marciniak SJ, Ron D, Przedborski S, Kholodilov N, Greene LA, Burke RE. CHOP/GADD153 is a mediator of apoptotic death in substantia nigra dopamine neurons in an in vivo neurotoxin model of parkinsonism. J Neurochem. Nov.2005 95:974. [PubMed: 16135078]

62. Parker WD Jr, Parks JK, Swerdlow RH. Complex I deficiency in Parkinson's disease frontal cortex. Brain Res. Jan 16.2008 1189:215. [PubMed: 18061150]

63. Keeney PM, Xie J, Capaldi RA, Bennett JP Jr. Parkinson's disease brain mitochondrial complex I has oxidatively damaged subunits and is functionally impaired and misassembled. J Neurosci. May 10.2006 26:5256. [PubMed: 16687518]

64. Morais VA, De Strooper B. Mitochondria dysfunction and neurodegenerative disorders: cause or consequence. J Alzheimers Dis. 20(Suppl 2):S255. [PubMed: 20463408]

65. Geisler S, Holmstrom KM, Skujat D, Fiesel FC, Rothfuss OC, Kahle PJ, Springer W. PINK1/Parkin-mediated mitophagy is dependent on VDAC1 and p62/SQSTM1. Nat Cell Biol. Feb. 12:119. [PubMed: 20098416]

66. Gentleman RC, Carey VJ, Bates DM, Bolstad B, Dettling M, Dudoit S, Ellis B, Gautier L, Ge Y, Gentry J, Hornik K, Hothorn T, Huber W, Iacus S, Irizarry R, Leisch F, Li C, Maechler M, Rossini AJ, Sawitzki G, Smith C, Smyth G, Tierney L, Yang JY, Zhang J. Bioconductor: open software development for computational biology and bioinformatics. Genome Biol. 2004; 5:R80. [PubMed: 15461798]
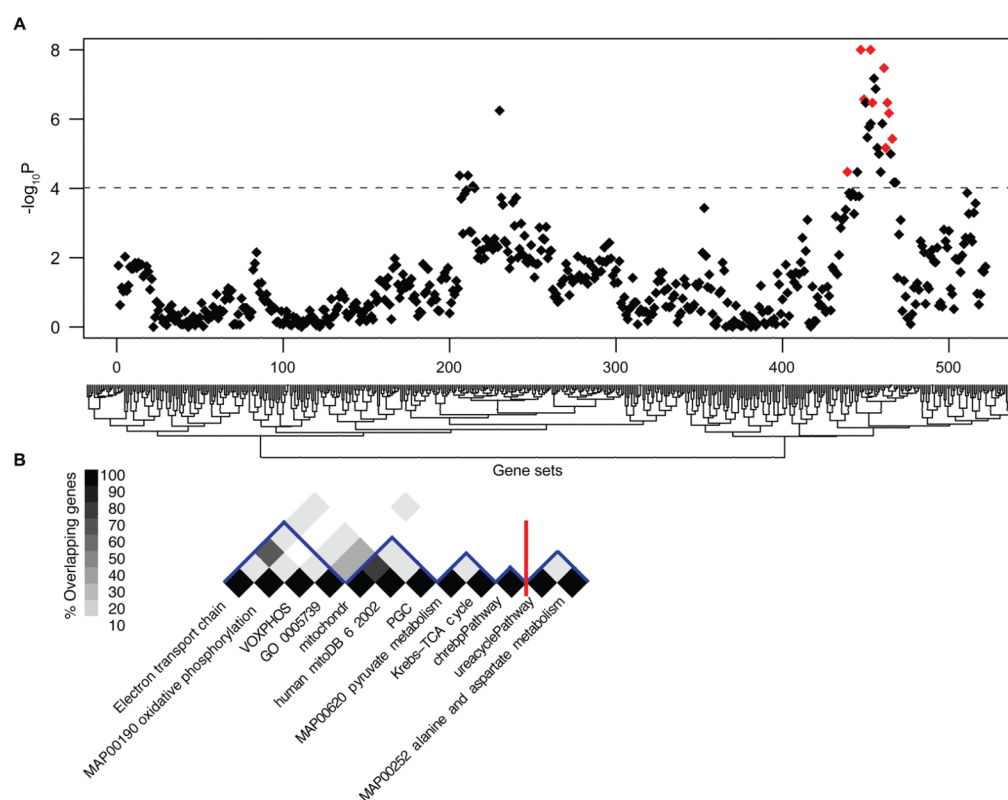
Fig. 1.

Association between 522 molecular gene sets and PD. (**A**) Random-effects meta-GSEA of 522 prespecified gene sets across nine genome-wide expression studies representing 185 laser-captured dopamine neuron and substantia nigra transcriptomes. Twenty-eight gene sets were associated with PD with genome-wide significance (*P* values $< 9.6 \times 10^{-5}$, corresponding to dashed line). Negative log-transformed *P* values indicating the significance of each of the 522 associations are shown on the y axis. Associations with PD were confirmed for 10 of the 28 gene sets in stage 2 and 3 analyses (Table 2) and are highlighted in red in (A). The 522 gene sets interrogated are displayed on the x axis and are clustered by their effect size estimate.

(**B**) Twelve gene sets were taken forward for replication to stages 2 and 3. These include 10 partially overlapping gene sets that were associated with PD at all three stages of analysis. The defects in cellular energetics detected by these gene sets include the distinct, but interconnected, processes of nuclear-encoded mitochondrial electron transport (ETC, MAP00190 oxidative phosphorylation, VOXPHOS, and GO 0005739), and *PGC-1α–*responsive mitochondrial bioenergetics (PGC, human mitoDB 6 2002, and mitochondr), glucose utilization (MAP00620 pyruvate metabolism and Krebs-TCA Cycle), and glucose sensing (ChREBP pathway). Two of the 12 gene sets forwarded across all stages, urea cycle pathway and MAP00252 alanine and aspartate metabolism, failed replication in stage 3. The percentage of genes overlapping between pairs of gene sets is color-coded on a grayscale. Gene set nomenclature and annotations correspond to version 1.1 of the MSigDB C2.
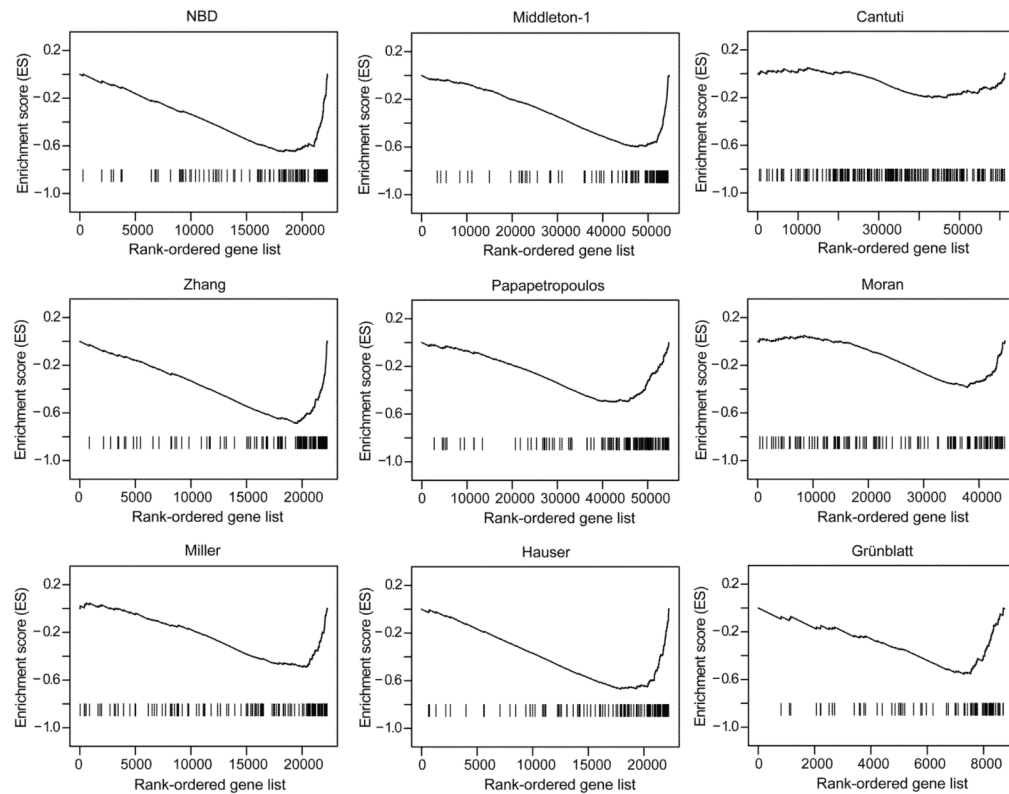
Fig. 2.
Enrichment plots (25) for the ETC gene set in the nine GWESs representing stage 1 of the pathway analysis. The lower portion ("barcode graph") of each plot shows probes for the thousands of target genes rank-ordered (left to right) by their differential expression in PD compared to controls (x axis). Ranks are based on the signal-to-noise ratio metric. Probes targeting genes overexpressed in patients with PD are top-ranked (near 1; left), and probes targeting genes underexpressed in patients with PD are low-ranked (near the end of the sorted gene list; right). The vertical lines show where probes for the 95 ETC genes appear in this ranked-ordered gene list. In most barcode graphs, visual inspection indicates that ETC genes are enriched at the end (right) of each rank-ordered list, consistent with a gene set that is underexpressed in PD. By contrast, in one of the nine GWESs (Cantuti), ETC genes appear randomly distributed across the sorted gene list, indicating that the ETC gene set is not enriched in this particular study.
The top portion of each plot shows the enrichment score (y axis) that is calculated by walking down the rank-ordered gene list from top- to last-ranked gene, decreasing a running-sum statistic when a gene is encountered that is not part of the ETC gene set, and increasing the score when a gene is encountered that is in the ETC gene set. Because ETC genes are underrepresented among the top ranks and enriched among the last ranks, highly negative maximal enrichment scores (distinct valleys) are achieved for ETC in most GWESs, consistent with a coordinated underexpression of the ETC pathway in PD.
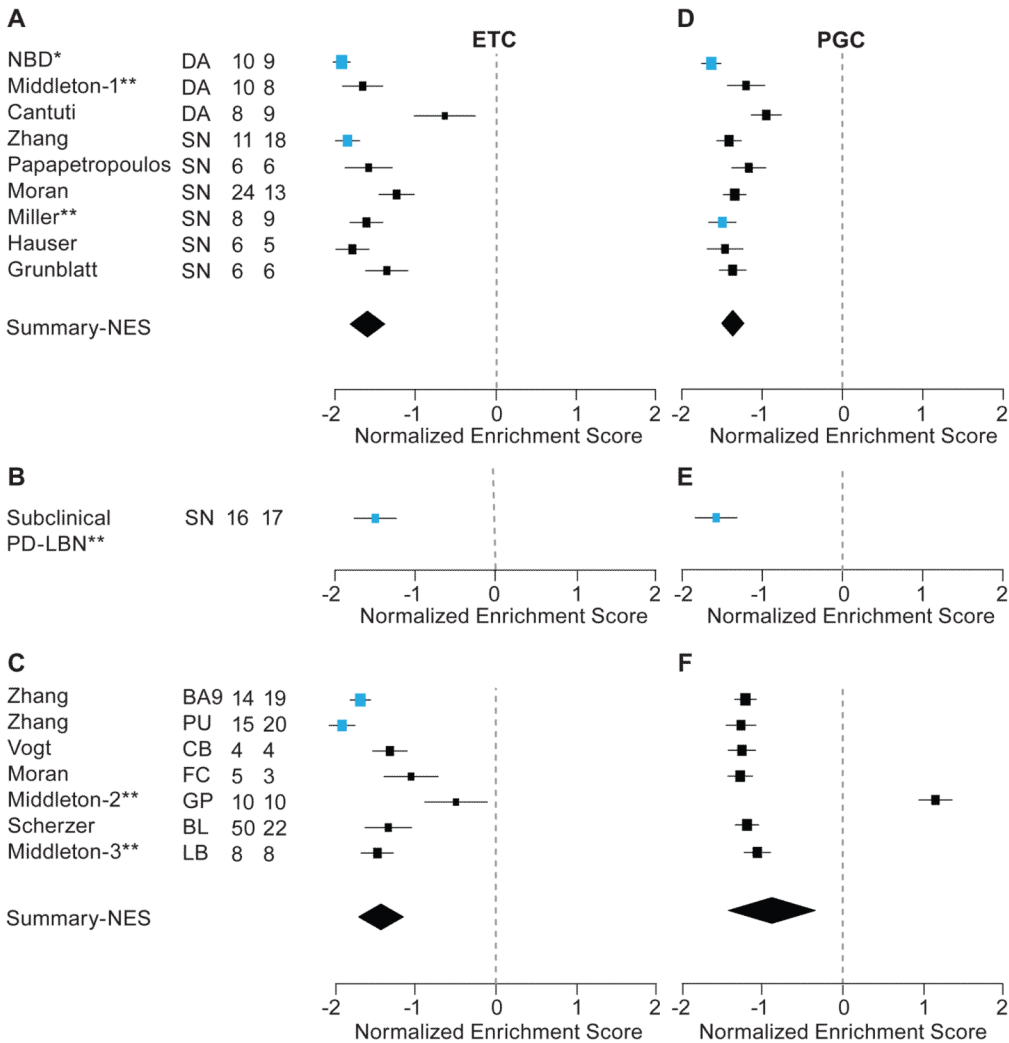
Fig. 3.
(**A** to **C**) Forrest plots of NES estimates (± SD) for the ETC gene set. To account for the size of each gene set, we normalized enrichment scores yielding the NES. The data are presented separately for each of the 17 studies. Blue squares, association ($P ≤ 0.05$) in an individual study; black squares, association ($P > 0.05$) in an individual study. The size of a square is inversely proportional to its respective SD. The summary estimate is indicated by a diamond; the width of the diamond is proportional to the 95% confidence interval of the sNES. **,previously unpublished studies; *,study unpublished at the time of analysis and since reported in (24).

(**A**) NES estimates for the ETC gene set in nine substantia nigra and laser-captured dopamine neuron GWESs representing a total of 185 transcriptomes (99 arrays from cases and 86 arrays from controls). Note that the third laser-captured dopamine neuron (DA) data set (Cantuti) is a technical outlier (see fig. S1).

(**B**) NES estimates for the ETC gene set in an analysis of postmortem substantia nigra of 16 individuals with subclinical PD-related Lewy body neuropathology (PD-LBN), and 17 age-, sex-, and PMI-matched controls.

(**C**) NES estimates for the ETC gene set in seven GWES, representing 192 extranigral transcriptomes or 106 arrays from cases and 86 from controls. These include brain regions that show abundant Lewy body pathology without appreciable neuron loss in PD, such as

FC and prefrontal cortex BA9, as well as basal ganglia structures that are affected by biochemical changes in PD such as GP and PU. One data set derived from human LB cell lines and one from cellular whole blood were included.

(**D to F**) NES estimates for the *PGC-1α* gene set. The data are presented separately for each of the 17 studies analyzed as above. Blue squares, association ($P \leq 0.05$) in an individual study.
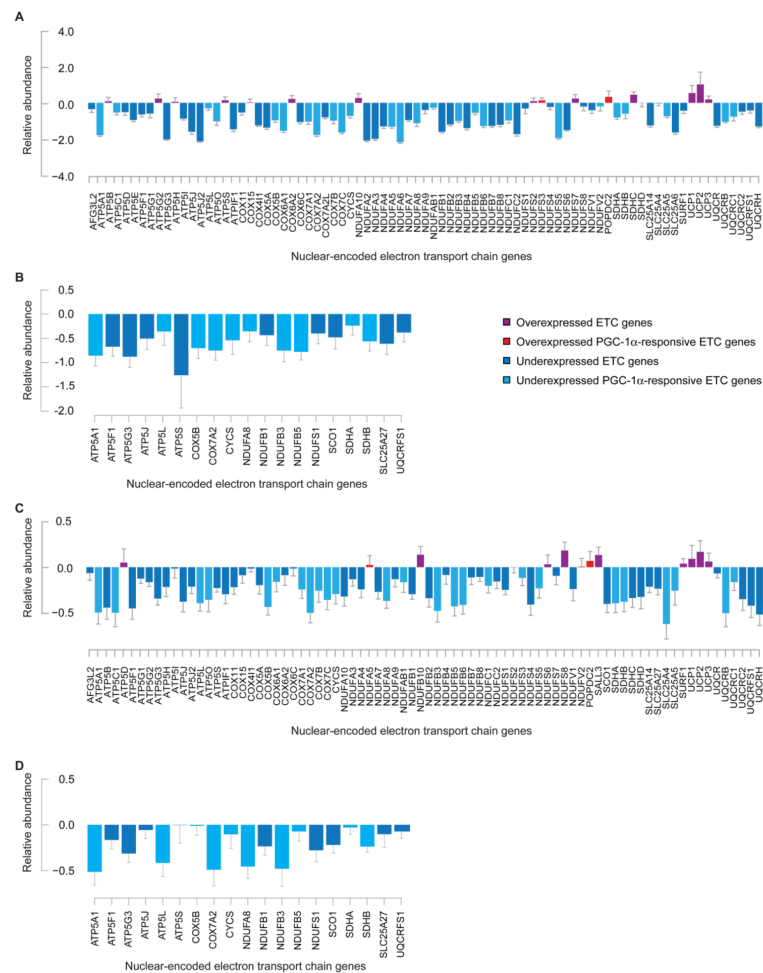
Fig. 4.

Nuclear-encoded ETC genes are coordinately underexpressed in laser-captured dopamine neurons of patients with PD and in the substantia nigra of individuals with incipient Lewy body disease.

(**A**) Most nuclear-encoded ETC genes are underexpressed in laser-captured dopamine neurons of patients with PD. ETC genes responsive to the master transcriptional regulator *PGC-1α* are color-coded in light blue (underexpressed) or bright red (overexpressed). Underexpression of other ETC genes is color-coded in dark blue and overexpression in purple. Data from the NBD GWES assayed on the Affymetrix platform are shown. For genes interrogated by multiple probes, results for only one probe are visualized due to space limitations (the median probe or a representative probe for odd or even numbers of probes, respectively).

(**B**) qPCR analysis confirms underexpression of select ETC genes in substantia nigra of patients with PD. Underexpression of ETC genes (dark blue) and a subset of *PGC-1α*–responsive ETC (light blue) was confirmed in 13 independent cases with PD and 17 age- and sex-matched controls by qPCR, with $P = 3.8 \times 10^{-6}$ and $P = 0.002$, respectively, by binomial test.

(**C**) Nuclear-encoded ETC genes are underexpressed in subclinical PD-related Lewy body neuropathology ($P = 0.015$). Expression changes were assayed on the Illumina platform. Select genes are interrogated by multiple probes. Note different scales in A and C.

(**D**) qPCR analysis confirms underexpression of select ETC genes in subclinical PD-related Lewy body neuropathology. Underexpression of ETC genes (dark blue) and a subset of *PGC-1α*–responsive ETC (light blue) was confirmed in subclinical PD-related Lewy body neuropathology by qPCR, with $P = 3.8 \times 10^{-6}$ and $P = 0.002$, respectively, by binomial test.
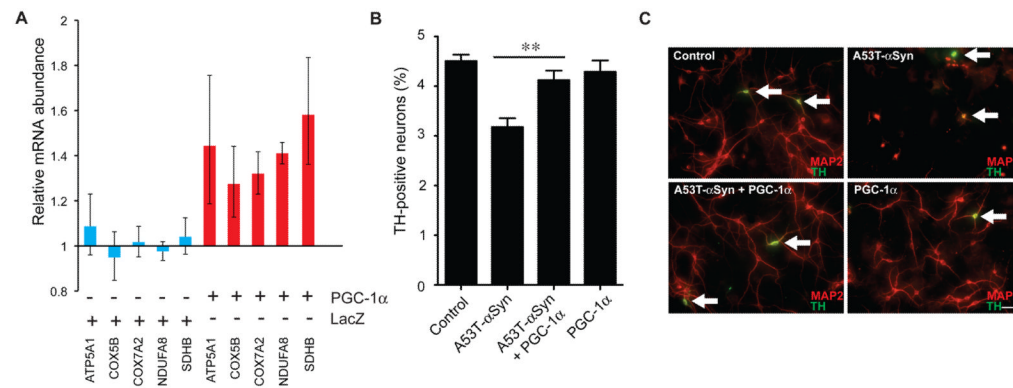
Fig. 5. *PGC-1α* coactivates nuclear-encoded electron transport genes and blocks α-synuclein–induced degeneration of dopaminergic neurons in rat primary midbrain cultures

(**A**) Cotransduction with adenovirus carrying human *PGC-1α* activated the expression of endogenous genes encoding nuclear subunits of the mitochondrial respiratory chain complexes I, II, IV, and V in rat midbrain primary neurons overexpressing A53T-α-synuclein (red bars). By contrast, transduction with the control gene *LacZ* did not materially affect expression of these genes in A53T–α-synuclein–expressing primary neurons (blue bars). The ribosomal gene *RPL13* was used to control for input RNA. Midbrain cultures transduced with A53T-α-synuclein alone were used as calibrator. Mean ± SEM are shown (N = 3 for each treatment).

(**B**) Human *PGC-1α* rescues preferential loss of TH-positive neurons induced by A53T–α-synuclein overexpression in rat midbrain primary cultures. Primary rat embryonic midbrain cultures were either mock infected (control) or transduced with adenovirus encoding A53T–α-synuclein alone, or both A53T–α-synuclein plus *PGC-1α,* or *PGC-1α* alone. Selective loss of dopamine neurons was assessed immunocytochemically by determining the percentage of MAP2-positive neurons that also stained positive for TH. **$P < 0.01$ by one-way analysis of variance (ANOVA) with Newman-Keuls post-hoc test. Mean ± SEM are shown (N = 3 for all treatments).

(**C**) *PGC-1α* overexpression antagonized α-synuclein–induced dopaminergic neuron loss and abrogated the A53T–α-synuclein–mediated retraction of MAP2- and TH-positive neuronal processes. Arrows, dopaminergic neurons positive for both MAP2 (red) and TH (green). Scale bar, 40 μm.
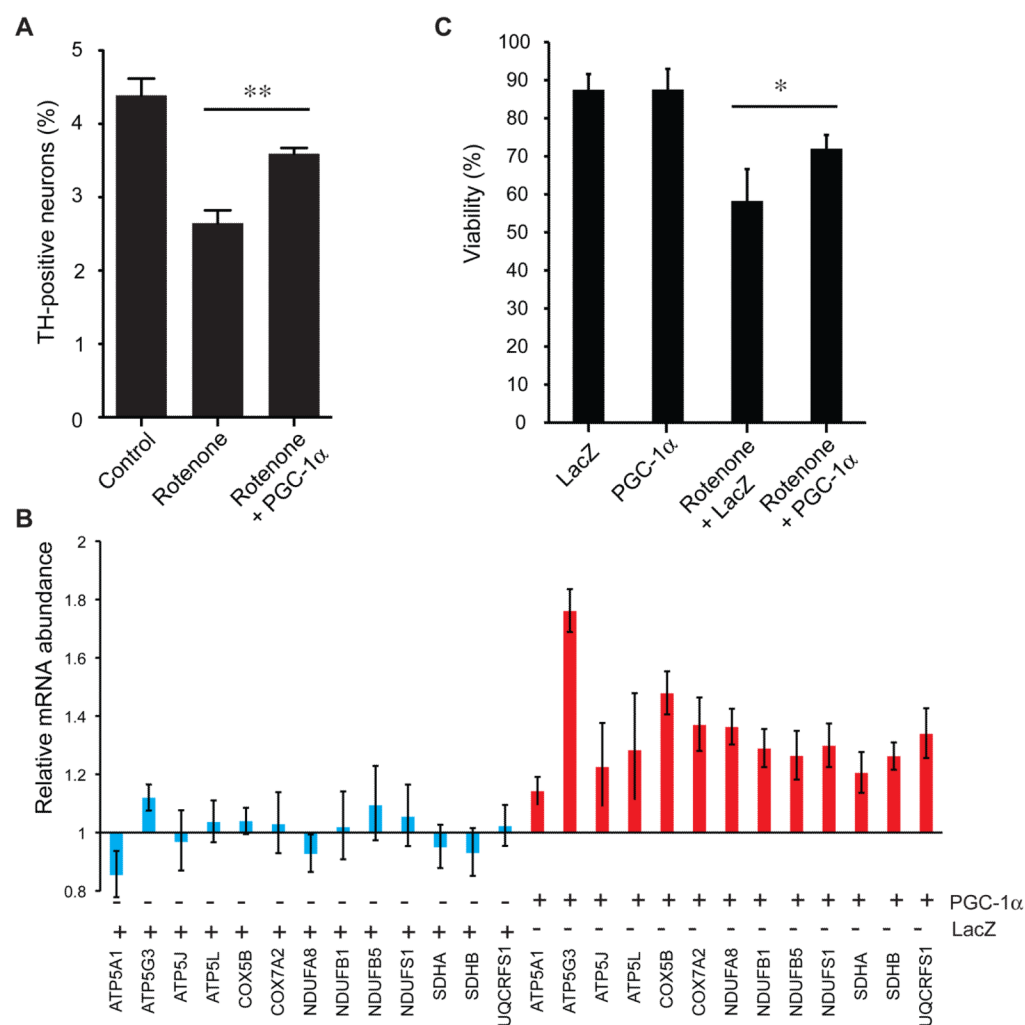
Figure 6. *PGC-1α* **suppresses loss of primary dopamine neurons and up-regulates nuclear subunits and viability in cellular models of rotenone toxicity**

(**A**) Transduction with adenovirus encoding human *PGC-1α* suppressed loss of TH-positive neurons induced by exposure to rotenone (100 nM) in primary mesencephalic cultures. **P < 0.01 by one-way ANOVA with Newman-Keuls post-hoc test. Mean ± SEM are shown (N = 4 for all treatments).

(**B**) *PGC-1α* over-expression in human catecholaminergic SH-SY5Y cells treated with rotenone (10 μM) coactivated the expression of nuclear-encoded subunits of complex I to V of the mitochondrial ETC (red bars) compared to gene expression in rotenone-treated cells transduced with the control gene *LacZ* (blue bars). The ribosomal gene *RPL13* was used to control for input RNA; untransfected cells treated with rotenone alone were used as calibrator. Mean ± SEM are shown (N = 3 to 4 for all treatments).

(**C**) Overexpression of *PGC-1α* compared to the control gene *LacZ* induced a small but statistically significant 14% increase in viability of human catecholaminergic SH-SY5Y cells treated with rotenone (10 μM) as estimated by the MTT assay. Percentage cell viability compared to untreated control cells is shown. *P = 0.02 by two-sided *t* test. Mean ± SEM are shown (N = 8 for all treatments).

Table 1

Overview of study design

Study	Country	Gene sets (n)	Probes (n)	RNA source	Cases			Controls		
					Number	Age at death (range)	% Male	Number	Age at death (range)	% Male
Stage 1					**99**	**77 (61–94)**	**64**	**86**	**72 (41–94)**	**61**
1	NBD*	USA	522	22,283	DA	10	78 (71–80+)	70	9	75 (61–80+)	67
2	Middleton-1**	USA	522	54,675	DA	10[a]	77 (63–93)	50	8[a]	67 (47–94)	38
3	Cantuti	USA	522	61,369	DA	8	73 (61–94)	63	9	71 (61–89)	44
4	Zhang	USA	522	22,283	SN	11[a]	75 (67–84)	54	18[a]	67 (41–94)	72
5	Papapetropoulos	USA	522	54,675	SN	16	74 (63–87)	81	9	81 (46–90)	44
6	Moran	UK	522	44,760	SN	24[b]	80 (68–89)	60	13[b]	69 (46–81)	86
7	Miller**	USA	522	22,283	SN	8	79 (70–84)[c]	NA	9	69 (52–84)[c]	NA
8	Hauser	USA	522	22,283	SN	6	82 (74–87)	66	5	81 (72–90)	20
9	Grünblatt	Israel	522	8,793	SN	6	77 (70–87)	33	6	79 (68–88)	83
Stage 2	Subclinical PD-LBN**	USA	28	48,803	SN	**16**	**83 (56–103)**	**50**	**17**	**75 (40–95)**	**53**
Stage 3					**106**	**72 (52–93)**	**68**	**86**	**69 (40–94)**	**64**
1	Zhang	USA	12	22,283	BA9	14[d]	77 (67–89)	57	19[d]	66 (41–94)	74
2	Zhang	USA	12	22,283	PU	15[d]	77 (67–89)	60	20[d]	66 (41–94)	75
3	Vogt	Germany	12	22,283	CB	4	83 (79–85)	75	4	85 (81–86)	75
4	Moran	UK	12	44,760	FC	5	78 (68–87)	60	3	72 (57–81)	100
5	Middleton-2**	USA	12	54,675	GP	10[d]	80 (63–93)	60	10[d]	79 (70–88)	70
6	Scherzer	USA	12	22,283	Blood	50	69 (52–86)	76	22	64 (40–80)	50
7	Middleton-3**	USA	12	54,675	LB	8	68 (65–73)	50	8	68 (65–72)	50
Stages 1–3					**221**[e]	**75 (52–103)**	**66**	**189**[e]	**72 (40–95)**	**59**

**
Unpublished;

*
unpublished at time of analysis and since reported (24); DA, laser-captured substantia nigra dopamine neurons; SN, substantia nigra; subclinical PD-LBN, subclinical, mild, PD-related Lewy body neuropathology; BA9, Broadman area 9; PU, putamen; CB, cerebellum; FC, frontal cortex; GP, globus pallidus internus; blood, whole cellular blood; LB, human lymphoblastoid cells;

[a] The sum of unique subjects analyzed across Middleton-1 and Zhang-SN (total of 14 unique patients with PD and 21 unique controls) differs from the sum of arrays because for a subset of participants SN homogenates as well as DA were assayed;

[b] 15 unique PD and 7 unique control subjects were assayed; for a subset of these individuals two arrays were assayed on medial and lateral substantia nigra, respectively;

[c] Age information was missing for some subjects;

[d] The sum of unique subjects analyzed across Zhang-BA9, Zhang-PU, Middleton-2 (total of 25 unique patients with PD and 30 unique controls) differs from the sum of arrays because arrays were assayed on multiple brain regions for a subset of participants;

[e] 172 unique patients with PD and 139 unique controls were assayed across stages 1–3.

Table 2

Twelve PD-associated gene sets taken forward to stages 2 and 3

Gene set #	N Genes	Annotation #	Stage 1 (DA & SN)		Stage 2 (Subclinical PD-LBN)		Stage 3 (non -SN)		All data			All SN data		
			sNES	P value	sNES	P value	sNES	P value	N	sNES	P value	N	sNES	P value
Electron transport chain	95	Broad	-1.583	$<1\times10^{-8}$	-1.496	1.46×10^{-2}	-1.420	1.66×10^{-5}	410	-1.519	$<1\times10^{-8}$	218	-1.580	$<1\times10^{-8}$
MAP00190 Oxidative phosphorylation	46	GenMAPP	-1.572	$<1\times10^{-8}$	-1.716	4.70×10^{-2}	-1.132	2.52×10^{-3}	410	-1.388	$<1\times10^{-8}$	218	-1.586	$<1\times10^{-8}$
MAP00620 Pyruvate metabolism	31	GenMAPP	-1.529	3.36×10^{-8}	-1.844	2.37×10^{-2}	-1.062	4.59×10^{-3}	410	-1.332	$<1\times10^{-8}$	218	-1.541	$<1\times10^{-8}$
VOXPHOS	87	BioCarta	-1.527	1.34×10^{-7}	-1.451	2.28×10^{-2}	-1.389	1.94×10^{-5}	410	-1.471	$<1\times10^{-8}$	218	-1.524	7.92×10^{-8}
Mitochondr	447	Broad	-1.464	6.76×10^{-7}	-1.761	1.43×10^{-2}	-1.247	5.21×10^{-4}	410	-1.376	$<1\times10^{-8}$	218	-1.479	5.54×10^{-7}
Krebs-TCA Cycle	29	BioCarta	-1.447	3.38×10^{-7}	-1.633	3.02×10^{-2}	-1.184	1.28×10^{-3}	410	-1.359	6.22×10^{-8}	218	-1.462	8.71×10^{-7}
Human mitoDB 6 2002	428	Broad	-1.427	3.38×10^{-7}	-1.750	1.23×10^{-2}	-1.271	4.21×10^{-4}	410	-1.373	$<1\times10^{-8}$	218	-1.445	5.32×10^{-7}
GO 0005739	170	GO	-1.369	3.72×10^{-6}	-1.758	2.04×10^{-2}	-1.230	5.87×10^{-4}	410	-1.322	3.11×10^{-8}	218	-1.391	3.19×10^{-6}
PGC	425	Broad	-1.366	6.75×10^{-6}	-1.576	4.96×10^{-2}	-0.884	1.65×10^{-2}	410	-1.165	6.32×10^{-7}	218	-1.379	2.93×10^{-6}
ChREBP pathway	20	Broad	-1.280	3.34×10^{-5}	-2.100	1.19×10^{-2}	-0.799	3.38×10^{-2}	410	-1.127	3.16×10^{-7}	218	-1.341	6.92×10^{-6}
Urea cycle pathway	7	KEGG	-1.262	6.77×10^{-5}	-1.671	1.46×10^{-2}	-0.575	1.15×10^{-1}	410	-0.994	0.00002212	218	-1.294	2.65×10^{-5}
MAP00252 Alanine and aspartate metabolism	21	GenMAPP	-1.165	3.39×10^{-5}	-1.831	1.80×10^{-2}	-0.482	1.91×10^{-1}	410	-0.908	0.00015813	218	-1.213	0.00018659

DA, GWES of laser-captured SN dopamine neurons; SN, substantia nigra GWES; GWES; subclinical PD-LBN, GWES of SN from individuals with subclinical, mild, PD-related Lewy body neuropathology;

gene set sources and gene set nomenclature correspond to version 1.1 of the MSigDB C2.